A simplified model for linear and nonlinear processes in thermoacoustic prime movers. Part I. Model and linear theory

M. Watanabe,[a] A. Prosperetti, and H. Yuan
Department of Mechanical Engineering, The Johns Hopkins University, Baltimore, Maryland 21218

(Received 12 December 1995; accepted for publication 30 July 1997)

A simplified quasi-one-dimensional model of thermoacoustic devices is formulated by averaging the conservation equations over the cross section. Heat transfer and drag effects are introduced by means of suitable coefficients. While the primary motivation for this work is the development of a model approximately valid in the nonlinear regime, the focus of this paper is the proper formulation of the transfer coefficients and the analysis of the linear problem. The accuracy of the model is demonstrated by comparison with existing more precise theories and data. Examples of devices with variable cross section demonstrate the flexibility of the approach. © *1997 Acoustical Society of America.* [S0001-4966(97)01412-4]

PACS numbers: 43.35.Ud [HEB]

INTRODUCTION

In recent years there has been a renewal of interest in thermoacoustic devices, both prime movers and heat pumps (for reviews see Wheatley, 1986; Swift, 1988). The foundations of the linear theory were firmly established in a well-known series of papers by Rott (1969, 1976, 1980, 1983, and others) and further developed by a number of authors (Merkli and Thomann, 1975; Yazaki *et al.*, 1980, 1987; Arnott *et al.*, 1991, 1992 1996; Atchley, 1992, 1994; Atchley and Kuo, 1994; Atchley *et al.*, 1990a, 1990b, 1992; Olson and Swift, 1994; Raspet *et al.*, 1993; Swift, 1992; Swift and Keolian, 1993; Wheatley *et al.*, 1983). As a consequence of this work, the linear analytical theory of such devices is now well developed although, due to the complexities of the process, it appears doubtful that much progress can be made into the nonlinear realm along similar lines (Gaitan and Atchley, 1993).

Progress in the direction of nonlinear phenomena clearly requires a time-domain formulation. For this purpose, we use a method very common in the study of nonlinear compressible flows and shock waves, namely the integration of the governing equations over the cross section of the device (see, e.g., Crocco, 1958; Landau and Lifshitz, 1959). This procedure leads us to a quasi-one-dimensional model that, although approximate, appears useful to further an understanding of thermoacoustic devices in the nonlinear regime.

Briefly, the novelty of the model described in this paper consists in: (i) its nonlinear nature; (ii) its formulation in the time domain necessary for the study of nonlinear effects; and (iii) its ability to account for changes of the cross section of the device also in the nonlinear regime.

In spite of its approximate nature, the present model is still very complex and its full study is a nontrivial matter. In the present paper we consider the prime mover case. We develop the model and compare it with the existing linear theory. Part II of this study (Yuan *et al.*, 1997) addresses the issue of the numerical integration of the nonlinear problem and presents some results. Future work will be devoted to improved approximations, the weakly nonlinear regime, the refrigerator case, and other related topics.

I. SIMPLIFIED MODEL OF THERMOACOUSTIC DEVICES

Most thermoacoustic devices consist of an acoustic resonator containing different heat transfer components (stack, heat exchangers, etc.). Typically the dimensions along the direction of the particle displacement, the resonator ''axis,'' is much longer than the transverse one and this circumstance suggests the basis for our approximation. We recast the governing equations in an integrated form over the cross section of the device thus reducing the model to one dimension in space (along the tube axis) and time. Effects taking place in the orthogonal directions (friction, heat transfer, etc.) are to be accounted for approximately by the introduction of suitable terms in the equations.

Consider a thermoacoustic device consisting of a duct of variable area $S(x)$. The coordinate x is taken along the axis of the device that is not necessarily straight. Upon integrating the equation of continuity over the volume delimited by two neighboring cross sections $S(x)$ and $S(x+dx)$ we find the well-known relation

$$\frac{\partial\langle\rho\rangle}{\partial t}+\frac{1}{S}\frac{\partial S\langle\rho u\rangle}{\partial x}=0, \tag{1}$$

where ρ is the gas density, u the velocity in the x direction, and the angle brackets indicate the cross sectional average,

$$\langle\cdots\rangle=\frac{1}{S(x)}\int_{S(x)}dS(\cdots). \tag{2}$$

The vanishing of the exact normal velocity on the lateral walls of the duct has been applied to obtain (1).

Similarly, the momentum equation in the x direction becomes

[a]Present address: Department of Mechanical Engineering, Kyushu University, 5-10-1 Hakozeki, Higashi-ku, Fukuoka, Japan 812.

$$\frac{\partial\langle\rho u\rangle}{\partial t}+\frac{1}{S}\frac{\partial}{\partial x}\left(S\langle\rho u^2\rangle\right)+\frac{\partial\langle p\rangle}{\partial x}+\frac{1}{S}\left(\langle p\rangle-\overline{p}\right)\frac{dS}{dx}$$

$$=-\frac{\mathscr{P}}{S}\left(\overline{\boldsymbol{\tau}\cdot\mathbf{n}}\right)_x. \tag{3}$$

Here, p is the gas pressure, $\boldsymbol{\tau}$ the viscous stress tensor, and the overline denotes the average over the ''wetted perimeter'' $\mathscr{L}$, i.e., the lines along which the cross-section S is cut by solid boundaries,

$$\overline{p}=\frac{1}{\mathscr{P}}\oint_{\mathscr{L}} p\ dl, \tag{4}$$

where $\mathscr{P}$ is the length of $\mathscr{L}$. The unit normal $\mathbf{n}$ is directed into the fluid region. The viscous component τ_{xx} has been neglected in deriving (3).

Before turning to the energy equation we introduce an assumption widely used in gas dynamics (see e.g., Crocco, 1958 for a discussion), namely that the fields are approximately uniform over the cross section. [The assumption of uniform pressure over the cross section has already been used in thermoacoustics, e.g., by Tominaga (1995) and can be traced at least as far back as Lord Rayleigh.] As a consequence of the cross-sectional uniformity, $\langle p\rangle\simeq\overline{p}$ and we may disregard correlation terms writing the average of products as products of averages. This approximation is addressed quantitatively in Sec. IV. The effects of nonuniformities, such as wall drag, are accounted for in an approximate manner. For the wall shear stress we write

$$\frac{\mathscr{P}}{S}\left(\overline{\boldsymbol{\tau}\cdot\mathbf{n}}\right)_x\equiv\mathscr{D}(u), \tag{5}$$

where $\mathscr{D}$ is a suitable operator the exact form of which can only be found in the linear case as shown later in Sec. III, Eq. (45). As made evident from this relation, in the linear domain, $\mathscr{D}(u)/\langle u\rangle$ is a complex, frequency-dependent quantity. The first feature implies that the wall drag has a component in phase with the velocity and one in phase with the acceleration, while the second one implies that an exact representation of the action of $\mathscr{D}(u)$ requires a convolution integral in time. The latter feature would render the integration of the equations over the many thousands of cycles necessary to reach steady state completely impractical. We are therefore forced to neglect memory effects assuming the form

$$\mathscr{D}(u)=\rho D\left[1+\theta_V\left(\frac{\partial}{\partial t}+\langle u\rangle\ \frac{\partial}{\partial x}\right)\right]\langle u\rangle, \tag{6}$$

where D and θ_V are quantities to be specified later. The latter parameter accounts for the phase relation between velocity and acceleration. Truncated to the linear terms, this form approximates the correct action of $\mathscr{D}$ in the case of single-frequency oscillations. The convective term $\langle u\rangle\partial\langle u\rangle/\partial x$ is an educated guess of a form suitable for the nonlinear regime. With these assumptions, and the omission henceforth of explicit indication of cross-sectional averages, the continuity (1) and momentum (3) equations become

$$\frac{\partial\rho}{\partial t}+\frac{1}{S}\frac{\partial}{\partial x}\left(S\rho u\right)=0, \tag{7}$$

$$\frac{\partial\rho u}{\partial t}+\frac{1}{S}\frac{\partial}{\partial x}\left(S\rho u^2\right)+\frac{\partial p}{\partial x}=-\mathscr{D}(u). \tag{8}$$

The cross-sectional averaging procedure applied to the energy equation of a perfect gas gives

$$\frac{\partial}{\partial t}\left[\frac{1}{\gamma-1}\,p+\frac{1}{2}\,\rho u^2\right]+\frac{1}{S}\frac{\partial}{\partial x}\left[uS\left(\frac{\gamma}{\gamma-1}\,p+\frac{1}{2}\,\rho u^2\right)\right]$$

$$=\frac{\mathscr{P}}{S}\,\overline{\mathbf{q}\cdot\mathbf{n}}, \tag{9}$$

where $\mathbf{q}$ is the heat flux and γ is the ratio of specific heats. The most intense heat transfer occurs in the directions normal to x and, accordingly, the effect of axial conduction q_x has been disregarded. This approximation is of course invalid at the ends of the tube. We return on this point below. Note also that the viscous dissipation term has been neglected here because it is small in comparison with the wall heat transfer.

Similar to (5), we introduce two heat transfer operators $\mathscr{H}$, $\mathscr{Q}$ by writing

$$\frac{\mathscr{P}}{S}\,\overline{\mathbf{q}\cdot\mathbf{n}}\equiv\mathscr{H}(T_w-T)-\frac{dT_w}{dx}\,\mathscr{Q}(u), \tag{10}$$

where $T_w(x)$ is the temperature of the solid structure (e.g., the stack plates) at x. In this paper this quantity is taken to be prescribed, e.g., on the basis of experiment. A refinement of the model enabling T_w to be calculated will be presented in a future paper. The second term in (10) accounts for the distortion of the temperature distribution due to the flow in the presence of a mean temperature gradient. This ansatz is suggested by the structure of the temperature distribution given by the exact linear theory as will be seen below in connection with Eq. (51). As for $\mathscr{D}$, the form for the operators $\mathscr{H}$, $\mathscr{Q}$ assumed here is

$$\mathscr{H}(T_w-T)=\rho c_p H\left[1+\theta_T\left(\frac{\partial}{\partial t}+u\ \frac{\partial}{\partial x}\right)\right](T_w-T), \tag{11}$$

$$\mathscr{Q}(u)=\rho c_p Q\left[1-\theta_Q\left(\frac{\partial}{\partial t}+u\ \frac{\partial}{\partial x}\right)\right]u, \tag{12}$$

where c_p is the gas specific heat at constant pressure. The time derivatives have been introduced for the same reason as previously in connection with $\mathscr{D}(u)$, i.e., to account for phase relations. The convective derivative in (11) is taken to operate on T_w-T, rather than T alone, as what matters physically is the temperature difference between the fluid particle and the solid structure it is in contact with. If a particle has moved from x to $x+udt$, it will ''see'' a temperature $T_w(x+udt)$ rather than $T_w(x)$. The determination of the parameters H, Q, θ_T, and θ_Q will be considered in Sec. III.

Now, upon using (7) and (8) to eliminate the time derivatives of ρ and u, the energy equation (9) becomes

$$\frac{\partial p}{\partial t}+u\frac{\partial p}{\partial x}+\frac{\gamma p}{S}\frac{\partial}{\partial x}(Su)$$

$$=(\gamma-1)\left[\mathscr{K}(T_w-T)-\frac{dT_w}{dx}\mathscr{Q}(u)+u\mathscr{D}(u)\right]. \tag{13}$$

The third term in the right-hand side represents the rate of conversion of mechanical to thermal energy by friction.

The last step to close the system (7), (8), (13) is to specify an equation of state. We assume that the averaged variables are related by the perfect gas equation

$$p=R\rho T, \tag{14}$$

where R is the universal gas constant divided by the gas molecular mass.

In Part II of this study (Yuan *et al.*, 1997), devoted to the nonlinear problem, it will prove desirable to change slightly the form of $\mathscr{K}$ shown above by adding a second-order spatial derivative. In this way it will be possible to bring the spectra of the approximate and exact linear problems in better agreement, which is important when nonlinearities cause a mixing of different modes. Since the remainder of this paper is devoted to the linear case, and for brevity, we postpone the discussion of this point until then.

In the present paper we consider only the prime mover problem in which the end walls of the tube are fixed. Therefore, we must require that the velocity vanish at $x=0$ and $x=L$. As a consequence of (8), this implies

$$\frac{\partial p}{\partial x}=0 \tag{15}$$

as well. Equations (7) and (13) written at the end points give then

$$\left[\frac{\partial \rho}{\partial t}+\rho\frac{\partial u}{\partial x}\right]_{x=0,L}=0, \tag{16}$$

$$\left[\frac{\partial p}{\partial t}+\gamma p\frac{\partial u}{\partial x}=\gamma\frac{p}{T}H\left(1+\theta_T\frac{\partial}{\partial t}\right)(T_w-T)\right]_{x=0,L}. \tag{17}$$

Upon eliminating $\partial u/\partial x$ one finds

$$\left[\frac{\partial}{\partial t}+H\left(1+\theta_T\frac{\partial}{\partial t}\right)\right]_{x=0,L}T$$

$$=\left[\frac{\gamma-1}{\gamma}\frac{T}{p}\frac{\partial p}{\partial t}+H\left(1+\theta_T\frac{\partial}{\partial t}\right)T_w\right]_{x=0,L}. \tag{18}$$

This relation shows that a knowledge of p at the boundary completely specifies the gas temperature perturbation provided T_w is known, as assumed in this paper. No additional boundary conditions are therefore necessary. In order to understand this result it may be useful to rewrite it in the exactly equivalent form

$$\frac{\partial}{\partial t}\left(\frac{T}{p^{\gamma-1/\gamma}}\right)=\frac{1}{p^{\gamma-1/\gamma}}H\left(1+\theta_T\frac{\partial}{\partial t}\right)(T_w-T), \tag{19}$$

which shows that the gas would behave adiabatically if H vanished, i.e., in the absence of heat exchange with the wall.

It is evident that, in general, the relation (18) implies a temperature jump at the left and right boundaries from the T given by this relation to the end-wall temperatures. This is a consequence of the neglect of axial conduction in the derivation of the energy equation (9). Axial conduction would introduce a term $\partial^2T/\partial x^2$, important only near the end walls, the role of which would be to reestablish continuity of temperature by means of a thin boundary layer. The temperature in this layer would adjust itself so as to match the value given by (18). This is an essentially passive process with negligible effects on the temperature distribution elsewhere in the device and can therefore be disregarded. Alternatively, the value of H at $x=0$, L can be adjusted to account for heat transfer with the terminations of the tube.

II. LINEARIZATION

The model described by Eqs. (7), (8), (13), and (14) is general. For the rest of this article we focus, however, only on its linear aspects.

We assume that, at equilibrium, the device contains gas at a uniform pressure p_0 and in thermal equilibrium with the solid boundaries with which it is in contact, so that its temperature is $T_w(x)$. Let now

$$p=p_0+p', \quad \rho=\rho_0+\rho', \quad T=T_w+T', \tag{20}$$

where the subscript 0 and the prime indicate unperturbed and perturbed quantities, respectively. The unperturbed quantities satisfy the equation of state with p_0 independent of x so that $\rho_0=\rho_0(x)$ must compensate for the x dependence of T_w. Upon assuming a time dependence proportional to $\exp i\omega t$ and neglecting quadratic and higher terms in the primed quantities and in u, we readily find:

$$i\omega\rho'+\frac{1}{S}\frac{d}{dx}(\rho_0 Su)=0, \tag{21}$$

$$\rho_0 i\omega u+\frac{dp'}{dx}=-\rho_0 D(1+i\omega\theta_V)u, \tag{22}$$

$$i\omega p'+\gamma\frac{p_0}{S}\frac{d(Su)}{dx}$$

$$=-\gamma\frac{p_0}{T_w}H(1+i\omega\theta_T)T'-(\gamma-1)\rho_0 c_p\frac{dT_w}{dx}$$

$$\times Q(1-i\omega\theta_Q)u. \tag{23}$$

From the momentum equation (22) we have

$$u=-\frac{1}{1+(1+i\omega\theta_V)(D/i\omega)}\frac{1}{\rho_0 i\omega}\frac{dp'}{dx}, \tag{24}$$

and, upon substituting into the continuity equation (21),

$$\rho'=-\frac{1}{\omega^2 S}\frac{d}{dx}\left[\frac{S}{1+(1+i\omega\theta_V)(D/i\omega)}\frac{dp'}{dx}\right]. \tag{25}$$

By substituting these relations into the energy equation (23) and using the linearized form of the equation of state we find the following equation for the pressure:

$$\frac{1}{S}\frac{d}{dx}\left[\frac{Sc_A^2}{1+(1+i\omega\theta_V)(D/i\omega)}\frac{dp'}{dx}\right]$$
$$+\omega^2 p'+\gamma\frac{H}{i\omega}(1+i\omega\theta_T)$$
$$\times\left\{\frac{c_I^2}{S}\frac{d}{dx}\left[\frac{S}{1+(1+i\omega\theta_V)(D/i\omega)}\frac{dp'}{dx}\right]+\omega^2 p'\right\}$$
$$+\frac{(\gamma-1)c_p}{1+(1+i\omega\theta_V)(D/i\omega)}\frac{dT_w}{dx}Q(1-i\omega\theta_Q)\frac{dp'}{dx}=0, \tag{26}$$

where

$$c_A^2=\gamma RT_w, \quad c_I^2=RT_w, \tag{27}$$

are the adiabatic and isothermal sound speeds, respectively. The associated boundary conditions are the vanishing of the first derivative at the two ends of the tube as given in Eq. (15).

If drag is disregarded so that $D=0$, the previous equation may be written in the time domain in the form

$$\frac{\partial}{\partial t}\left[\frac{1}{S}\frac{\partial}{\partial x}\left(Sc_A^2\frac{\partial p'}{\partial x}\right)-\frac{\partial^2 p'}{\partial t^2}\right]+\gamma H\left(1+\theta_T\frac{\partial}{\partial t}\right)$$
$$\times\left[\frac{c_I^2}{S}\frac{\partial}{\partial x}\left(S\frac{\partial p'}{\partial x}\right)-\frac{\partial^2 p'}{\partial t^2}\right]+(\gamma-1)c_p\frac{dT_w}{dx}Q$$
$$\times\left(1-\theta_Q\frac{\partial}{\partial t}\right)\frac{\partial^2 p'}{\partial x\,\partial t}=0. \tag{28}$$

This equation may be considered as falling in the class of the ''wave hierarchies'' studied, among others, by Whitham (1974). This remark is, however, of limited usefulness as the standard theory of wave hierarchies applies to propagating, rather than standing, waves.

Once the pressure has been found, the temperature disturbance can be calculated by eliminating $\partial(Su)/\partial x$ between the continuity and the energy equation. The result is

$$\left[1+\frac{H}{i\omega}(1+i\omega\theta_T)\right]T'$$
$$=\frac{p'}{\rho_0 c_p}+i\frac{u}{\omega}[1+Q(1-i\omega\theta_Q)]\frac{dT_w}{dx}. \tag{29}$$

With (24) for u and (25) for ρ', the determination of p' gives then a complete solution of the problem.

It is evident from (28) that, if no heat transfer occurs so that $H=0$, $Q=0$, the equation describes adiabatic sound waves in an imposed temperature distribution. In the opposite limit of very large heat transfer, but again with $Q=0$, the waves propagate isothermally in the sense that each fluid ''slice'' retains the temperature of the solid surface in contact with it. More generally, Eq. (28) describes the competition of processes occurring on three time scales, the acoustic one of the wave oscillation, that associated to heat transfer, and that associated to convection. These time scales can be estimated as follows. Let

$$\overline{c}, \quad \overline{H}, \quad \overline{T_w} \tag{30}$$

be suitable average values of the sound speed, heat transfer coefficient, and gas temperature. Then the acoustic time scale t_a is of order $\omega^{-1}\sim L/\overline{c}$, while for the thermal time scale, from the coefficient of the second group of terms in (28), we have

$$t_h\sim\frac{1}{\gamma\overline{H}}. \tag{31}$$

From the definition (11) of H we can clearly write

$$\rho c_p\overline{H}\Delta T\sim\frac{1}{l}k\frac{\Delta T}{\delta_K}, \tag{32}$$

where ΔT is of the order of the temperature difference between gas and solid surfaces in the stack, k is the gas thermal conductivity, δ_K defined by

$$\delta_K=\sqrt{\frac{2\alpha}{\omega}}, \tag{33}$$

with α the thermal diffusivity of the gas is the thermal diffusion length, and l is the plate spacing in the stack. Upon substitution into (31) we thus have

$$t_h\sim\frac{l\delta_K}{\gamma\alpha}, \tag{34}$$

The ratio of the thermal and acoustic time scales is then

$$\frac{t_h}{t_a}\sim\frac{l}{\gamma\delta_K}. \tag{35}$$

At low frequencies δ_K is large and the motion in the stack is dominated by the terms multiplied by H in (28). At high frequencies, the terms in the first square brackets prevail.

For the coefficient Q, it is simple to obtain the estimate $Q\sim 1$ so that, in order of magnitude, the ratio between the first and the last group of terms of (28) is

$$\frac{(\gamma-1)c_p Q(dT_w/dx)(\partial^2 p'/\partial x\,\partial t)}{c_A^2(\partial^3 p'/\partial x^2\,\partial t)}\sim\frac{T_H-T_C}{\overline{T_w}}\frac{L}{L_S}, \tag{36}$$

where T_H-T_C is the temperature difference over the length L_S of the stack. This estimate indicates that this convective term is not small in typical applications.

Viscous effects introduce an additional time scale $t_v\sim 1/D$ that affects equally the ''isothermal'' and the ''adiabatic'' components. From the definition (6) we expect that $D\sim\nu/l\delta_V$, where ν is the gas kinematic viscosity and δ_V the viscous diffusion length defined by

$$\delta_V=\sqrt{\frac{2\nu}{\omega}}=\sqrt{\sigma}\delta_K, \tag{37}$$

with σ the Prandtl number. The condition for viscous effects to be negligible is that $t_v\omega\ll 1$, which is verified at low frequencies. Since, for gases, diffusivities are of the order of the speed of sound times the molecular mean free path s (see, e.g., Chapman and Cowling, 1952), we have

$$\omega t_v\sim\frac{l}{L}\frac{\delta_V}{s}. \tag{38}$$

This quantity can assume a wide range of values depending on pressure, temperature, and nature of the gas. The ratio of t_h and t_v is

$$\frac{t_h}{t_v} \sim \frac{1}{\gamma}\frac{\nu}{\alpha}\frac{\delta_K}{\delta_V} = \frac{\sqrt{\sigma}}{\gamma}. \tag{39}$$

Since the Prandtl number has a value close to 1 for most gases, this relation implies that viscous effects are normally just as important as heat transfer ones.

III. DRAG AND HEAT TRANSFER PARAMETERS

In the linear regime, appropriate expressions for the drag and heat transfer coefficients can be found from their definitions (6) and (10) upon comparison with the exact linear results.

Swift (1988, Eq. A4) gives the following expression for the velocity field in a plane channel of width l:

$$u_1 = \frac{i}{\omega\rho_0}\frac{dp'}{dx}\left(1 - \frac{\cosh(1+i)y/\delta_V}{\cosh(1+i)l/2\delta_V}\right), \tag{40}$$

where y is measured from the center plane of the channel and the diffusion length δ_V is given by (37). From this equation we have

$$(\boldsymbol{\tau}\cdot\mathbf{n})_x = -\mu\left.\frac{\partial u_1}{\partial y}\right|_{y=l/2} = -\frac{i(1+i)\mu}{\omega\rho_0\delta_V}\frac{dp'}{dx}\tanh\frac{(1+i)l}{2\delta_V}. \tag{41}$$

The mean velocity in the channel (to be identified with our u) is

$$u = \frac{1}{l}\int_{-l/2}^{l/2} u_1\, dy = \frac{i}{\omega\rho_0}(1-f_V)\frac{dp'}{dx}, \tag{42}$$

where

$$f_V = \frac{\tanh(1+i)l/2\delta_V}{(1+i)l/2\delta_V}. \tag{43}$$

From these two expressions we find

$$\frac{\mathscr{P}}{S}(\overline{\boldsymbol{\tau}\cdot\mathbf{n}})_x = -i\omega\rho_0\frac{f_V}{1-f_V}u. \tag{44}$$

Comparison with (6) then gives

$$D(1+\omega\theta_V) = i\omega\frac{f_V}{1-f_V}. \tag{45}$$

Upon separating real and imaginary parts, explicit expressions for D and θ_V are readily obtained.

For later reference it is useful to note the following asymptotic behaviors of the function $f_V(\eta)$, with $\eta = 2\delta_V/l$, defined by (43). In the thin viscous layer limit $\eta \to 0$ and one has

$$f_V \simeq \tfrac{1}{2}(1-i)\eta, \tag{46}$$

while, for $\delta_V \gg l$,

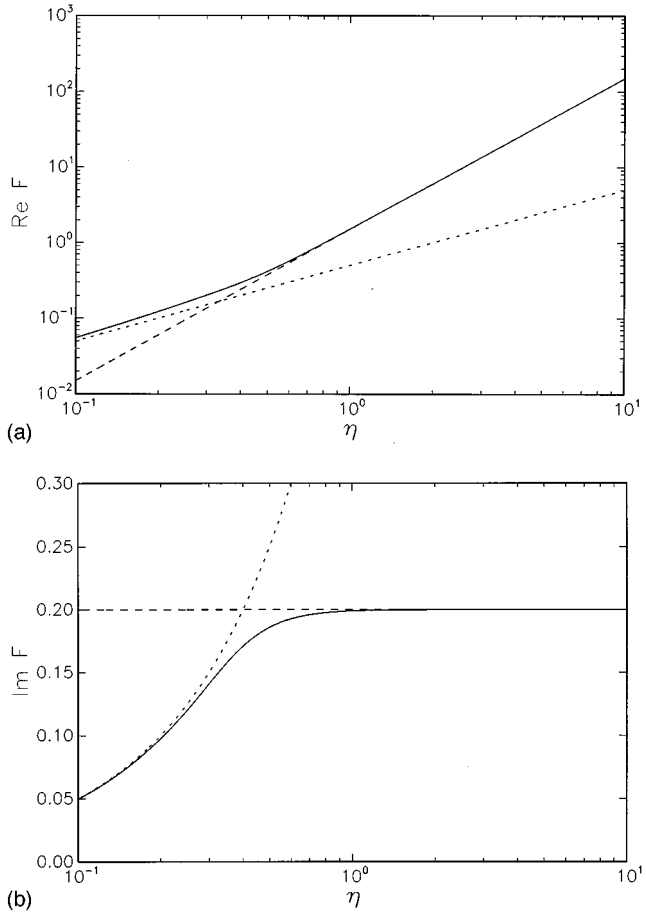

FIG. 1. The real, (a), and imaginary, (b), parts of the function $F(\eta)$ defined in (48). The dashed line is the asymptotic approximation (50) for $\eta \to \infty$, and the dotted line the approximation (49) for $\eta \to 0$ truncated to the term linear in η.

$$f_V \simeq 1 - \frac{2i}{3\eta^2} - \frac{8}{15\eta^4}. \tag{47}$$

With these results it is easy to establish the asymptotic behavior of

$$F = \frac{if_V}{1-f_V}, \tag{48}$$

namely

$$F \simeq \tfrac{1}{2}(1+i)\eta + \tfrac{1}{2}\eta^2 + \tfrac{1}{4}(1-i)\eta^3, \quad \eta \to 0, \tag{49}$$

and

$$F \simeq \frac{3}{2}\eta^2 + \frac{i}{5} - \frac{338}{175}\frac{1}{\eta^2}, \quad \eta \to \infty. \tag{50}$$

Graphs of the real and imaginary parts of F are shown in Fig. 1.

We now proceed in a similar fashion to calculate the heat transfer coefficient. From Eq. (A10) in Swift (1988), neglecting the small term ϵ_s involving the conductivity and heat capacity of the solid, we have the temperature perturbation in the channel as

$$T_1=\frac{p'}{\rho_0 c_p}\left[1-\frac{\cosh(1+i)y/\delta_K}{\cosh(1+i)l/2\delta_K}\right]+\frac{1}{\omega^2\rho_0}\frac{dp'}{dx}\frac{dT_w}{dx}\left[\frac{\sigma}{\sigma-1}\frac{\cosh(1+i)y/\delta_V}{\cosh(1+i)l/2\delta_V}-\frac{1}{\sigma-1}\frac{\cosh(1+i)y/\delta_K}{\cosh(1+i)l/2\delta_K}-1\right], \tag{51}$$

where the thermal diffusion length δ_K has been defined in (33). The structure of this result, with dependence on both δ_V and δ_K, shows that the temperature disturbance is determined by both convection and conduction processes. This is the reason for our ansatz (10) to express the mean energy transport.

Using (51), we can calculate the mean of T_1 over the channel width, to be identified with the temperature disturbance T' of our theory:

$$T'=(1-f_K)\frac{p'}{\rho_0 c_P}+\frac{1}{\omega^2\rho_0(1-\sigma)}\times[\sigma(1-f_V)-(1-f_K)]\frac{dT_w}{dx}\frac{dp'}{dx}, \tag{52}$$

where, as in (43),

$$f_K=\frac{\tanh(1+i)l/2\delta_K}{(1+i)l/2\delta_K}. \tag{53}$$

Again from (51), one can calculate the heat flux into the boundaries:

$$-\overline{\mathbf{q}\cdot\mathbf{n}}=\frac{kl}{\delta_K^2}\left[if_K\frac{p'}{\rho_0 c_p}+\frac{f_V-f_K}{(1-f_V)(1-\sigma)}\frac{dT_w}{dx}u\right]. \tag{54}$$

Upon using (42) and (52), we then find

$$-\frac{\mathscr{P}}{S}\overline{\mathbf{q}\cdot\mathbf{n}}=\frac{i\omega k}{\alpha}\frac{f_K}{1-f_K}T'+\frac{k}{\alpha(1-\sigma)}\frac{dT_w}{dx}\times\left(\sigma-1+\frac{1}{1-f_v}-\frac{\sigma}{1-f_K}\right)u, \tag{55}$$

from which, comparing with (11) and (12), we deduce

$$H(1+i\omega\theta_T)=i\omega\frac{f_K}{1-f_K}, \tag{56}$$

$$Q(1-i\omega\theta_Q)=\frac{1}{1-\sigma}\left(\frac{1}{1-f_V}-\frac{\sigma}{1-f_K}\right)-1. \tag{57}$$

The functions f_V, f_K defined in (43), (53) are appropriate for a plane channel geometry. As shown by Rott (1969), for a circular tube with radius r_0 one has

$$f_V=2\frac{J_1((i-1)(r_0/\delta_V))}{(i-1)(r_0/\delta_V)J_0((i-1)(r_0/\delta_V))}, \tag{58}$$

with a corresponding expression for f_K. Asymptotic approximations for large and small tube radii now are, with $\eta=2\delta_V/r_0$,

$$f_V\simeq\tfrac{1}{2}(1-i)\eta, \tag{59}$$

and

$$f_V\simeq 1-\frac{i}{2\eta^2}-\frac{1}{6\eta^4}, \tag{60}$$

respectively. Note that the two asymptotic expressions for small η are the same for the plane channel and the cylindrical tube. More generally, the same expression holds provided η is defined as the ratio of $2\delta_V$ to the hydraulic radius.

Upon substituting (45), (56), and (57) into the wave equation (26), we find

$$\frac{1}{S}\frac{d}{dx}\left[(1-f_V)S\frac{dp'}{dx}\right]+\frac{1}{T_w}\frac{dT_w}{dx}\left(1+\frac{\sigma f_V-f_K}{1-\sigma}\right)\frac{dp'}{dx}+\frac{\omega^2}{c_A^2}[1+(\gamma-1)f_K]p'=0. \tag{61}$$

If S is a constant, this equation is identical to that given by Swift [1988, his Eq. (54)] provided his wall parameter ϵ_s is neglected and the gas is treated as perfect. If the spatial variation of S is retained, it coincides with a result given by Rott [1976, his Eq. (6)]. With the choices (45), (56), and (57), the present theory thus reproduces exactly the eigenfrequency and pressure eigenfunction of the standard linear theory. The velocity and temperature eigenfunction are only reproduced in the cross-sectional mean as indicated by (42) and (52).

Upon substituting (45) for D into the expression (24) for u, we recover (42) as expected. The expression (29) for the (cross-sectional mean) temperature disturbance becomes

$$T'=\frac{1-f_K}{\rho_0 c_p}p'+\frac{i}{1-\sigma}\left(\frac{1-f_K}{1-f_V}-\sigma\right)\frac{u}{\omega}\frac{dT_w}{dx}=\frac{1-f_K}{\rho_0 c_p}p'-\frac{1}{\rho_0\omega^2}\left(1+\frac{\sigma f_V-f_K}{1-\sigma}\right)\frac{dT_w}{dx}\frac{dp'}{dx}, \tag{62}$$

while from (25) for the density disturbance we find

$$\rho'=-\frac{1}{\omega^2 S}\frac{\partial}{\partial x}\left[(1-f_V)S\frac{\partial p'}{\alpha x}\right]. \tag{63}$$

Upon substitution of the expression (56) for the heat transfer parameter into the linearized boundary condition (18) for the temperature we find

$$\frac{T'}{T_w}=(1-f_K)\frac{\gamma-1}{\gamma}\frac{p'}{p_0}. \tag{64}$$

This relation is identical to (62) evaluated at the end walls where $u=0$.

When the stack plates are widely separated, from (43) and (53), we have f_V, $f_K\simeq 0$ and as a consequence, from (57), $Q\simeq 0$. The temperature disturbance (62) becomes then

$$T'=\frac{1}{\rho_0 c_p}p'-\frac{1}{\rho_0\omega^2}\frac{\partial T_w}{\partial x}\frac{dp'}{dx}. \tag{65}$$

Setting the right-hand side to zero we find the well-known expression of the critical temperature gradient (see, e.g., Swift, 1988):

$$\left.\frac{d\overline{T_w}}{dx}\right|_{\text{crit}}=\frac{\omega^2 p'}{c_p(dp'/dx)}. \tag{66}$$

In general, however, only the component of T' in phase with the second term of Eq. (62) can be made to vanish by a suitable choice of dT_w/dx. The component in quadrature with this term will not normally be zero. We conclude that, in general, the gas temperature disturbance cannot vanish.

The procedure followed in this section has led to expressions for the viscous and heat transfer terms of the approximate model that match those of the exact linear theory for oscillations at one fixed frequency. Thus in the linear case where the different modes can be considered independently of each other, results such as Eq. (61) are exact. For example, Eq. (61) can be solved exactly to produce eigenfrequencies and eigenfunctions for all the modes. If many modes are present at the same time, as with a time-dependent nonlinear calculation, the need to use one specific value for each of the exchange parameters forces one to make some compromises. It turns out that in most practical cases only the lowest-frequency mode is unstable, and it is therefore reasonable to use the frequency of this mode to evaluate the parameters. The (real part of this) frequency can be approximated by

$$\overline{\omega}=\frac{\overline{c}}{L}, \tag{67}$$

where $\overline{c}=(\gamma R\overline{T_w})^{1/2}$ and

$$\overline{T_w}=\frac{1}{L}\int_0^L T_w(x)dx. \tag{68}$$

We will make use of $\overline{\omega}$ thus defined in some of the examples that follow. An unwelcome feature of committing oneself to one value of the frequency is, however, that the spectrum of the linear problem is altered. We shall pursue this point in Part II of this study devoted to the nonlinear problem (Yuan *et al.*, 1997).

The dependence of the boundary layer thicknesses (37), (33) on $\sqrt{\omega}$ implies that the diffusive transfers of momentum and energy to the solid boundaries are affected by the history of the flow and are therefore nonlocal in time. This feature is of course well recognized in the literature (see, e.g., Achard and Lespinard, 1981). The representations of the exchange operators assumed in (6), (11), and (12) are local in time and therefore can only be approximations. Conceivably, these approximations can be improved in the manner suggested by Achard and Lespinard by introducing, in place of explicit relations such as (10), differential ones connecting the time derivative of **q**, in addition to **q** itself, to the quantities in the right-hand side. In this way a nonlocal nature in time would be reintroduced, if with a kernel different from the exact one. This matter will be examined in a future study.

IV. CORRELATION TERMS

As pointed out in Sec. I, the major approximation underlying the present model consists in the neglect of the correlation terms, i.e., in setting the cross-sectional average of the product of two quantities equal to the product of the averages. Of course, the error associated with this procedure only affects the nonlinear calculations to be reported in subsequent papers as the choice of the drag and heat transfer parameters made in the previous section insures that the linear results are reproduced exactly. Nevertheless this remains an important point that we can examine approximately using exact linear-theory results such as (40) and (51).

The most interesting quantity to consider is the product u_1T_1 as it enters in the expression for the energy flow in the device (see, e.g., Rott, 1975; Swift, 1988). In the special case of $\sigma=1$, $dT_w/dx=0$, the result of this calculation also gives the correlation term for u_1^2. It may be noted that the neglect of correlation terms can be expected to be much more accurate for products involving the pressure field as, contrary to velocity, temperature, and density, the latter does not have a boundary layer structure.

By using (40) and (51), a straightforward calculation gives

$$\begin{aligned}\langle u_1T_1\rangle &\equiv \frac{1}{l}\int_0^l dy\ u_1(y)T_1(y)\\ &=\frac{i}{\omega\rho_0^2c_p}\,p'\,\frac{dp'}{dx}\,\Phi_e(\zeta,\sigma)\\ &\quad+\frac{i}{(1-\sigma)\omega^3\rho_0^2}\left(\frac{dp'}{dx}\right)^2\frac{dT_w}{dx}\,\Psi_e(\zeta,\sigma),\end{aligned} \tag{69}$$

where

$$\zeta=\frac{l/2}{\delta_V} \tag{70}$$

is the ratio of the channel half-width to the boundary layer thickness and

$$\Phi_e=1+\frac{\sigma f_V-f_K}{1-\sigma}, \tag{71}$$

$$\begin{aligned}\Psi_e&=1-\sigma+\frac{1}{2}\,\sigma\,\frac{5-3\sigma}{1-\sigma}\,f_V-\frac{1}{1-\sigma}\,f_K\\ &\quad-\frac{\sigma}{2\cosh^2(1+i)(l/2\delta_V)}.\end{aligned} \tag{72}$$

Here f_V and f_K are as defined in the previous section, Eq. (43), and we use the subscript e to indicate that these are exact expressions.

By taking the product of the averages (42) and (52) of u and T' we find an expression with the same structure as (69), but with the following approximate values of Φ and Ψ:

$$\Phi_{\text{app}}=(1-f_V)(1-f_K), \tag{73}$$

$$\Psi_{\text{app}}=(1-\sigma+\sigma f_V-f_K)(1-f_V). \tag{74}$$

It may be noted that, for $\sigma=0$, the boundary layer structure of the velocity field disappears and the exact and approximate expressions of Φ and Ψ become identical for any δ_K.

Figures 2 and 3 show the real and imaginary parts of the ratios Φ_e/Φ_{app} and Ψ_e/Ψ_{app} for $\sigma=0.71$ (helium) and $\sigma=0.392$ (60% helium and 40% argon mixture), respectively, as functions of $\zeta=(l/2)/\delta_V$. The range of interest of ζ for existing thermoacoustic engines with a gas medium is typically from a low value of 4 to 5 in the stack region to many tens or more away from the stack. The figures show that,

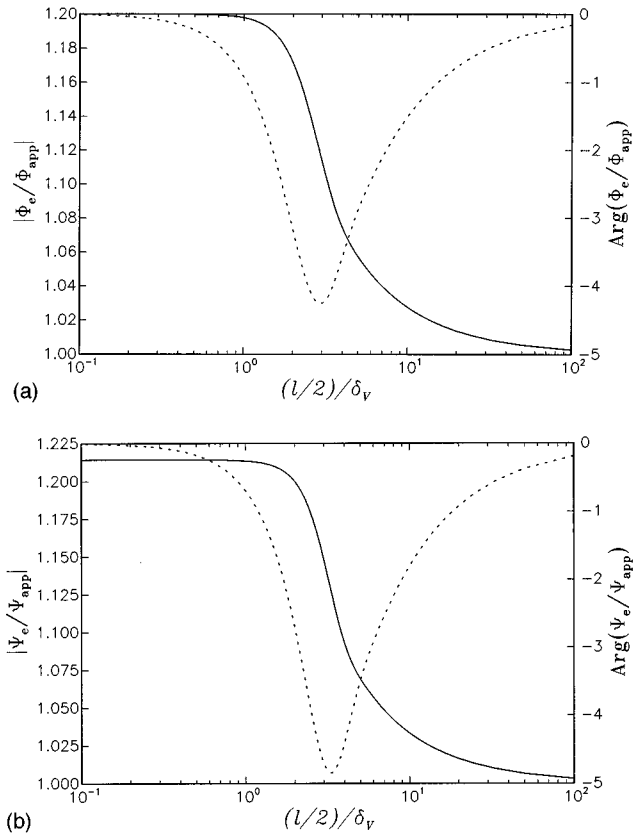

FIG. 2. The ratios $\Phi_e/\Phi_{\mathrm{app}}$, (a), and $\Psi_e/\Psi_{\mathrm{app}}$, (b), of the correlation coefficients appearing in the approximate and exact expressions of the velocity-temperature correlation (69) as functions of the ratio of the viscous penetration length δ_v to the channel half-width $\frac{1}{2}l$ for $\sigma=0.71$ (helium). The solid lines are the modulus and the dashed lines the argument in degrees. The range of interest of the ratio $(l/2)/\delta_v$ for existing thermoacoustic engines with a gas medium is typically from a low value of 4 to 5 up.

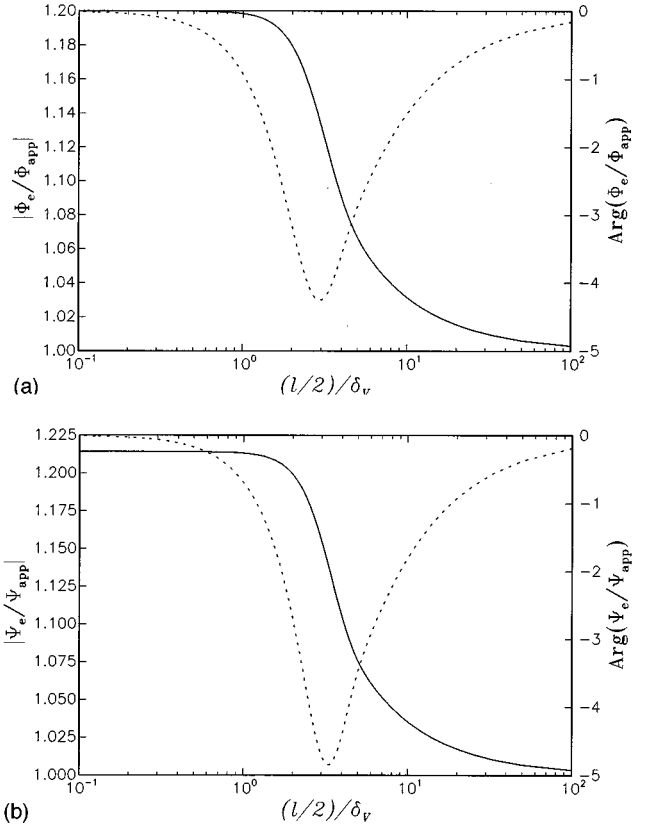

FIG. 3. The ratios $\Phi_e/\Phi_{\mathrm{app}}$, (a), and $\Psi_e/\Psi_{\mathrm{app}}$, (b) of the correlation coefficients appearing in the approximate and exact expressions of the velocity-temperature correlation (69) as functions of the ratio of the viscous penetration length δ_v to the channel half-width $\frac{1}{2}l$ for $\sigma=0.392$ (60% helium and 40% argon mixture). The solid lines are the modulus and the dashed lines the argument in degrees. The range of interest of the ratio $(l/2)/\delta_v$ for existing thermoacoustic engines with a gas medium is typically from a low value of 4 to 5 up.

over this range, the moduli of the approximate and exact expressions differ by less than 6% and the phases by less than 5°.

These results suggest that the negative impact of cross-sectional averaging is limited. In particular, the model should be able to reproduce correctly the trends of real thermoacoustic prime movers resulting from different values of parameters or operating conditions.

V. NUMERICAL RESULTS

We now turn to some numerical results obtained from the linearized equations of Sec. II. The expressions for the drag and heat transfer parameters found in Sec. III are used throughout. Although obtained from the linear theory, results of the type considered here do not seem to have been shown before. Most of the previous studies, and in particular the analysis of data that we consider here, have been based on approximations rather than on the exact theory.

As another point, we want to demonstrate the ability of the model to deal with devices with a variable cross section. By assuming a linear growth of the cross-sectional area with distance from $x=0$, we could readily adapt our model to the case of a cylindrical resonator. Since, however, a cylindrical system can be treated exactly by separation of variables, as recently demonstrated by Arnott *et al.* (1996), we prefer to focus on cases for which no exact method is available to demonstrate the specific strengths of our approach in this particular respect. For this reason, we consider a linear device with a contraction or expansion at its midsection.

We start by comparing the results of the model with the data of Atchley (1992) who measured the damping of oscillations in a thermoacoustic tube for different values of the imposed temperature difference across the stack. His results are expressed in terms of the inverse quality factor $1/Q$ of the oscillations that is related to the real and imaginary parts of the eigenfrequency ω appearing in our analysis by

$$\frac{1}{Q}=2\,\frac{\mathrm{Im}\ \omega}{\mathrm{Re}\ \omega}. \tag{75}$$

Below the stability threshold $1/Q$ is positive, while it becomes negative above. At the threshold, $1/Q=0$.

The gas used in the experiment was helium. Over the temperature range of interest here, from 300 to 650 K, we fit thermal conductivity data (Vargaftik, 1975) by a linear function of temperature as $k=0.151+3.228\times10^{-4}(T-300)$, with k in W/m K and T in K, which provides a better fit than a power law. We have included this effect in our calculation as the value of k determines the boundary layer thickness,

and therefore the heat transfer parameters. For the specific heat we use the constant value 5.2 kJ/kg K and $\gamma=5/3$, $\sigma=0.71$.

For Atchley's experiment, the tube length was 99.87 cm, its radius was 3.82 cm, the stack length $L_S=3.5$ cm, and the stack was positioned at $x_S=87.95$ cm from the cold end. The cold heat exchanger, consisting of two equal parts separated by 1.04 mm and 10.2-mm long, is to the left of the stack and the hot heat exchanger, 7.62-mm long, to the right. The combined cross-sectional area of the stack plates was 3.1 cm^2, i.e., 27% of the entire cross section. Atchley reports that the temperature was approximately constant and equal to its cold and hot values to the left and right of the stack, respectively, and linear in the stack so that $T=T_C$ for $0\leqslant x\leqslant x_S$, $T=T_H$ for $x_S+L_S\leqslant x\leqslant L$, and

$$T=T_C+\frac{x-x_S}{L_S}(T_H-T_C), \tag{76}$$

for $x_S<x<x_S+L_S$.

To solve Eq. (61) numerically we multiply by S and discretize by centered differences on an equispaced grid. This procedure requires the values of $(1-f_V)S$ at the half-integer nodes, that are calculated as simple arithmetic averages. Typically 2000 cells were used along the tube length, with approximately 100 in the stack region. The eigenvalues were searched by the inverse iteration method (Press *et al.*, 1992).

The specification of the cross-sectional area and wall temperature according to the data given before leads to strong spatial discontinuities of the cross section and heat flux. In principle this causes no difficulties, as Eq. (61) is in conservation form and the corresponding jump conditions on p' are automatically satisfied. However, such discontinuities cannot give a realistic representation of the actual physical situation. Small-scale thermal transport processes (conduction between the stack ends and the heat exchangers, natural convection, etc.) must cause the wall temperature distribution to become smoother than the mathematical idealization given by (76). Similarly, flow separation phenomena must prevent the streamlines from precisely expanding to follow the discontinuities of the cross-sectional area mentioned before. Unfortunately the published information does not give a characterization of the system sufficiently precise to enable us to use more realistic distributions. Therefore we decided to mimic the action of these unknown, but certainly present, diffusive processes by smoothing the discontinuous distributions of $S(x)$ and $T_w(x)$. We accomplish this by effecting a series of sweeps in which S_i and T_{wi}, the values of $S(x)$ and $T_w(x)$ at the node x_i, are replaced by

$$\tfrac{1}{4}(S_{i+1}+2S_i+S_{i-1}), \tag{77}$$

and similarly for T_w. The same prescription is applied to the exchange parameters D, H, Q, θ_V, θ_K, and θ_Q. It will be seen that this smoothing procedure has a rather strong impact on the final results. A comparison between the smoothed and nonsmoothed distributions is shown graphically in Part II for one example. It may be remarked that something corresponding to our smoothing operation is implicit in all earlier treatments of the problem where it is introduced (with limited control) through the spatial discretization.

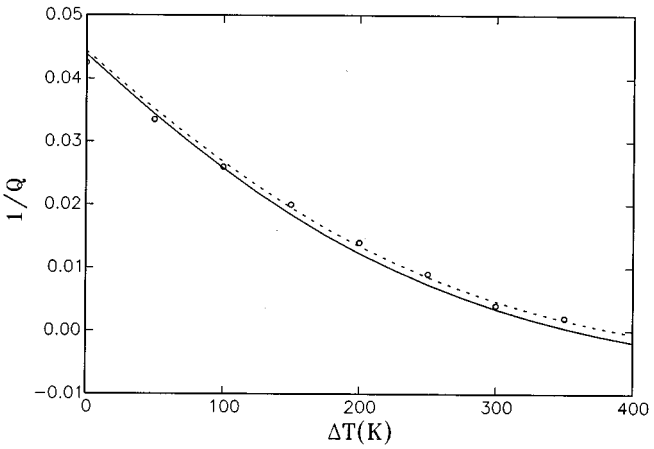

FIG. 4. $1/Q$ versus the temperature difference $\Delta T=T_H-T_C$ along the stack for an undisturbed pressure of 170 kPa. The circles are the data of Atchley (1992). The solid line is the result for discontinuous cross-sectional area and wall temperature distributions given in the text. The dashed line is the result with the same quantities smoothed by effecting the operation (77) 50 times.

Figures 4 and 5 show $1/Q$ versus the temperature difference $\Delta T=T_H-T_C$ along the stack for pressures of 170 and 500 kPa, respectively. The data are shown by circles. The solid lines are the result given by the full solution of the eigenvalue problem associated with Eq. (61) with the discontinuous area and temperature distributions as mentioned before. The dashed lines are the results corresponding to smoothed distributions with the smoothing procedure explained before applied 50 times in Fig. 4 and 200 times in Fig. 5.

Since Eq. (61) coincides with the exact linear theory, these results are to be considered exact solutions to the problem. In the past, the same data had only been analyzed on the basis of approximations to the eigenfunction and real part of the eigenfrequency (Atchley, 1992). It can be seen that, particularly in the unstable region where the temperature differ-

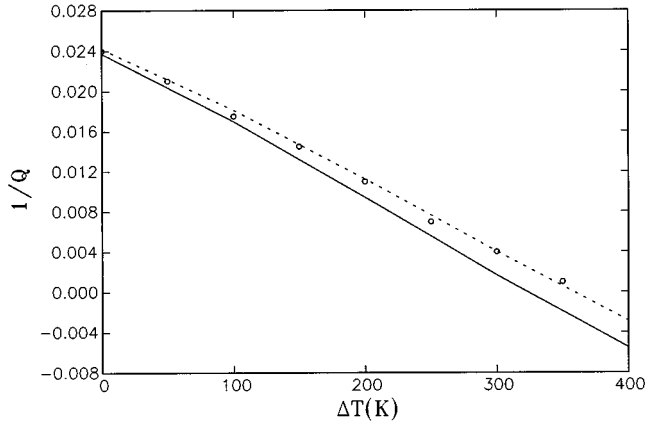

FIG. 5. $1/Q$ versus the temperature difference $\Delta T=T_H-T_C$ along the stack for an undisturbed pressure of 500 kPa. The circles the data of Atchley (1992). The solid line is the result for discontinuous cross-sectional area and wall temperature distributions given in the text. The dashed line is the result with the same quantities smoothed by effecting the operation (77) 200 times.

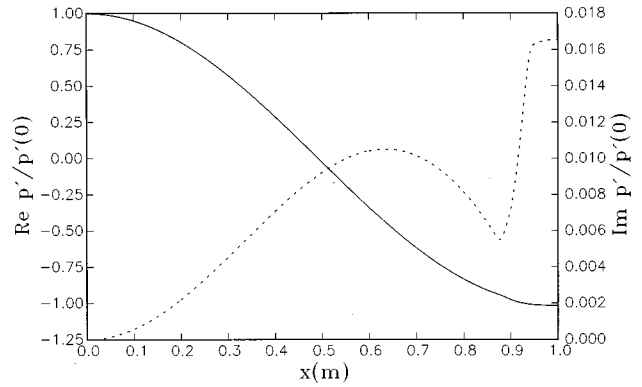

FIG. 6. Real (solid line) and imaginary part of the pressure eigenfunction for $\Delta T=350$ K, $p_0=500$ kPa, and the situation of Atchley's (1992) experiment.

ence is large, the smoothing has a significant effect on the results. By smoothing only the wall temperature or only the cross-sectional area, it is found that the latter affects the Q value more than the former. In both figures, and particularly at the higher pressure and temperatures, the data lie above the Q values calculated from the discontinuous distributions (solid lines). The smoothed distributions (dashed lines) give instead larger Q values and results generally closer to the data. The implication is that the thermoacoustic energy conversion process is stronger in the case of sharp discontinuities. At the higher pressure the density is larger and the effect of area discontinuities on the mass flux correspondingly greater. Of course, our smoothed profiles are simply a conjecture about the conditions prevailing in the experiment. Other causes may produce a larger Q, i.e., a greater damping. One may mention the mismatch between the number of plates in the heat exchangers and in the stack, or other factors as discussed by Atchley (1992). In spite of these elements of uncertainty, however, theory and experiment seem to be in good overall agreement. Only smoothed distributions are used in the calculations shown in the rest of the paper.

Figures 6 and 7 show the real and imaginary part of the normalized pressure and velocity eigenfunctions for $\Delta T=350$ K, $p_0=500$ kPa. The quantities plotted are

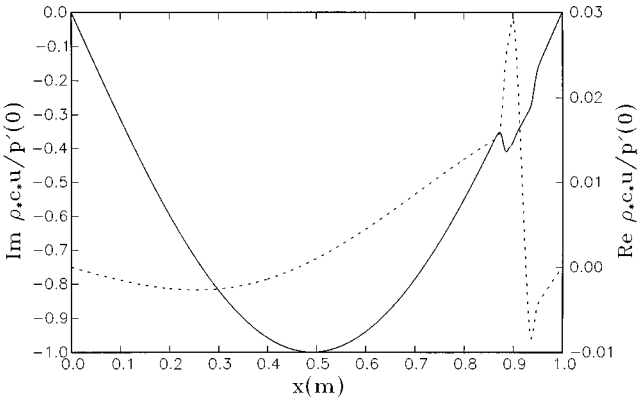

FIG. 7. Imaginary (solid line) and real part of the normalized velocity eigenfunction for $\Delta T=350$ K, $p_0=500$ kPa, and the situation of Atchley's (1992) experiment. The oscillations in the stack region occur in correspondence of the area changes.

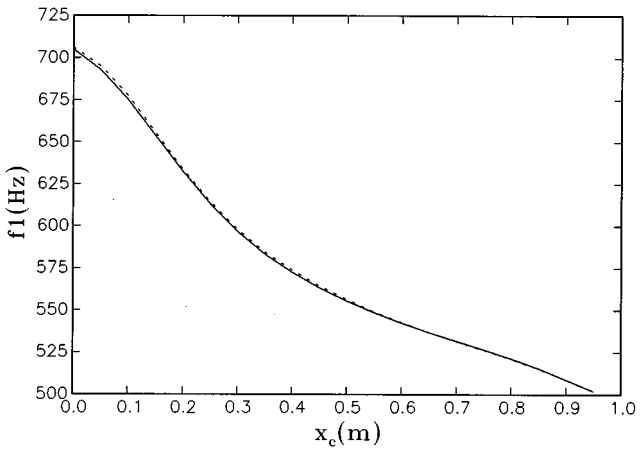

FIG. 8. Real part of the eigenfrequency of the fundamental mode $f_1=\mathrm{Re}\,\omega/2\pi$ as a function of the position of the cold end of the stack at 170 kPa for $\Delta T=300$ K. Other conditions as in Atchley's (1992) experiment. The gas temperature equals T_C in the entire region to the left of the stack and T_H to the right. In the stack region a linear dependence is assumed. The solid line is the exact result. The dashed line is obtained by using the approximation (67) for the parameter $\overline{\omega}$ entering the expression of the expression of the exchange coefficients D, H, and Q.

$$\frac{p'(x)}{p'(0)},\quad \frac{u'(x)\rho_* c_*}{p'(0)}=\frac{p_0}{p'(0)}\sqrt{\frac{\gamma}{RT_C}}\,u'(x). \tag{78}$$

The real part of p' (solid line, Fig. 6) and the imaginary part of u' (solid line, Fig. 7) are very close to the corresponding results for an unobstructed isothermal tube. The quantity affected most is the velocity, where the fluctuations in the stack region correspond to the rapid area variations. The imaginary part of p' and real part of u' (dashed lines) are much smaller.

Figure 8 is the real part of the eigenfrequency $\mathrm{Re}\,\omega/2\pi$ as a function of the position of the cold end of the stack, at a pressure of 170 kPa for $\Delta T=300$ K. The solid line is the exact value, and the dashed line the value calculated by approximating the exchange coefficients in terms of the effective angular frequency $\overline{\omega}$ defined in (67). The approximation is seen to be quite good. The significant change in the frequency is due to the fact that, in this calculation, the gas temperature has been taken equal to T_H in the entire region to the right of the stack.

Information on $\mathrm{Im}\,\omega$ as a function of the stack position is given in Fig. 9 in the form of a graph of $1/Q$ for 170 and 500 kPa and $\Delta T=300$ K. The solid lines are the exact results and the dashed lines those obtained by using $\overline{\omega}$ in the exchange coefficients. The system is seen to be most unstable for a stack position in the neighborhood of the 3/4 point as is well known (see, e.g., Swift, 1988). For this example, the lower pressure leads to a stronger maximum growth rate of the instability.

We now turn to a system with a cross-sectional area given by

$$S(x)=S_0\left[1+C\,\cos^2\,\pi\left(\frac{2x}{L}-1\right)\right]^2,$$

$$\text{for}\ \ \tfrac{1}{4}L\leqslant x\leqslant\tfrac{3}{4}L, \tag{79}$$

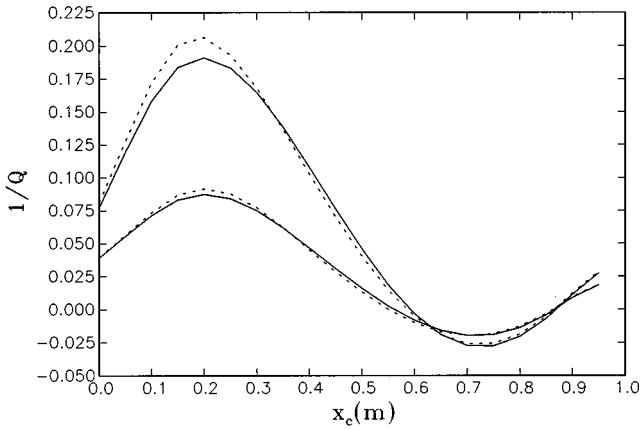

FIG. 9. $1/Q$ as a function of the stack position at two pressures from the exact linear theory with $\Delta T = 300$ K for Atchley's (1992) experiment. The dotted lines are the approximations due to the use of $\overline{\omega}$ defined in (67) in the expressions of the exchange coefficients D, H, and Q. The system is most unstable for a stack position in the neighborhood of the 3/4 point. The pair of lines with the smallest oscillation is for 500 kPa, the other pair for 170 kPa.

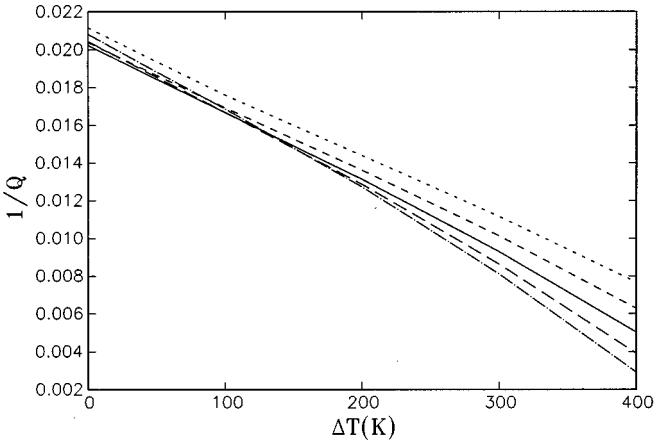

FIG. 11. Effect on the damping parameter $1/Q_2$ of the first harmonic mode of a narrowing or expanding cross section of the tube. ——— $C=0$, constant cross section; – – $C=0.2$; – · – · $C=0.4$; --- $C=-0.2$; · · · · · $C=-0.4$.

while $S=S_0$ elsewhere other than in the stack region which is the same as before. With $S_0=24$ cm^2 and $C=0$, this is the same system considered up to now. With $C>0$, the tube's cross section is thicker in the central region, and with $C<0$ it is thinner. The stack region has the same geometry as before independently of the value of C. Figures 10–12 show the effect of the cross-sectional area change on the Q value of the fundamental mode, the first, and the second harmonic. In all the figures, the dashed line is for $C=0$, the dotted line for the smallest value of C considered, $C=-0.4$, and the dash- dot line for the largest one, $C=0.4$. It is seen that thicker and thinner cross sections, respectively, increase and decrease the frequency of the fundamental and second harmonic, while they have the opposite effect on the first harmonic. The dependence of the corresponding frequencies on the temperature difference along the stack is rather weak, increasing with the order of the harmonic.

The Q value tends to become negative, implying instability, at smaller ΔT's for a thickening cross section than for a thinning one for the fundamental and first harmonic mode. A thickening cross section, however, has a stabilizing effect on the third harmonic at the higher ΔT's. These results can be interpreted by considering the eigenfunctions, two examples of which are shown in Figs. 13 and 14 for the fundamental mode. In all cases, the pressure distribution (solid line, left vertical scale) is very similar to the usual sinusoidal one. There is, however, a marked effect on the velocity distribution (dashed line, right vertical scale) as a consequence of the constraint arising from mass conservation. With a narrowing tube, the velocity is relatively large in the narrow part and has a long distance over which to decrease to zero at the left and right boundaries. It is therefore small in the stack region with a consequent reduction in the thermoacoustic effect. For a thickening cross section, on the other hand, the velocity starts decreasing closer to the ends, and therefore it is larger in the stack region. Another feature evident from these figures is the asymmetry, caused by the stack, of the

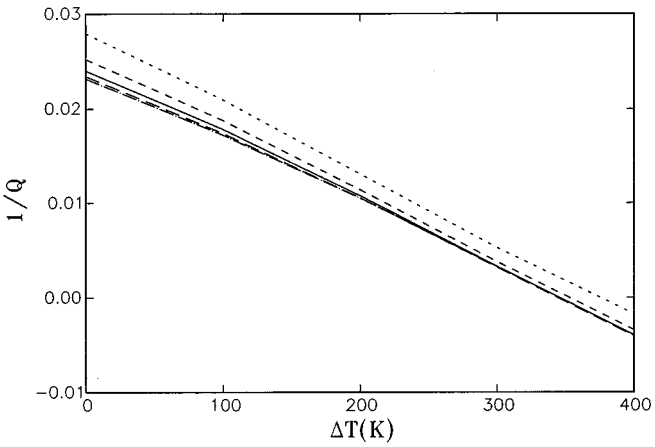

FIG. 10. Effect on the damping parameter $1/Q_1$ of the fundamental mode of a narrowing or expanding cross section of the tube. ——— $C=0$, constant cross section; – – $C=0.2$; – · – · $C=0.4$; --- $C=-0.2$; · · · · · $C=-0.4$.

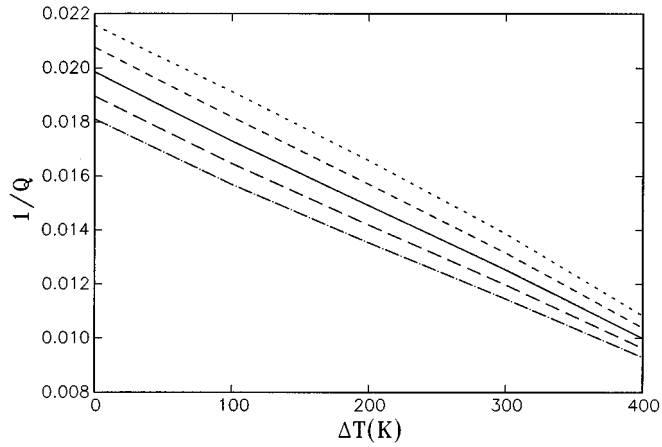

FIG. 12. Effect on the damping parameter $1/Q_3$ of the second harmonic mode of a narrowing or expanding cross section of the tube. ——— $C=0$, constant cross section; – – $C=0.2$; – · – · $C=0.4$; --- $C=-0.2$; · · · · · $C=-0.4$.

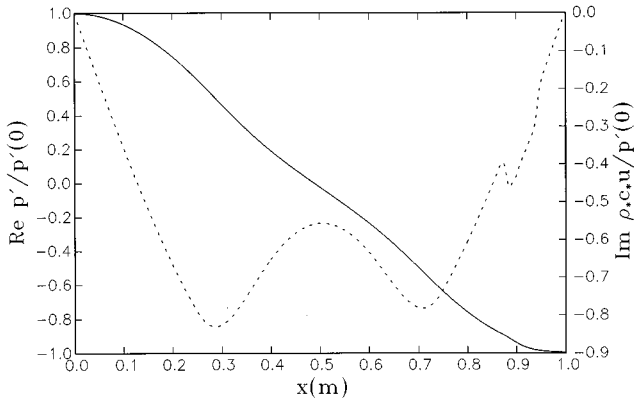

FIG. 13. Real part of the pressure eigenfunction (solid line, left vertical scale) and imaginary part of the normalized velocity eigenfunction (dashed line, right vertical scale) for a thickening tube with $C=0.2$; $\Delta T=350$ K and $p_0=500$ kPa.

velocity eigenfunction with respect to the tube's midpoint. It is found that, the larger ΔT, the steeper the eigenfunction near the hot end. Similar trends are found in the eigenfunctions of the first harmonic mode. For the second mode, however, the stack is close to the optimal position of 1/4 wavelength from the velocity node. Therefore for ΔT greater than about 500 K, the thickening of the cross section causes the antinode to move toward the stack thus decreasing the magnitude of the thermoacoustic destabilization. Conversely, narrowing the cross section displaces the antinode in the favorable direction and decreases the damping. The opposite occurs at lower ΔT's due to interplay between this effect and the asymmetrical nature of the eigenfunction.

As a final item of interest we show in Fig. 15 the ratios f_2/f_1 (solid line) and f_3/f_1 as a function of the cross-sectional area parameter C in Eq. (79) for $\Delta T=300$ K and a pressure of 500 kPa. For a straight tube $C=0$ and these ratios are extremely close to 2 and 3, respectively. Evidently, the detuning of the system resulting from the presence of the stack and of the heated region has a very small effect on the harmonic structure of the modes. Area changes do, however,

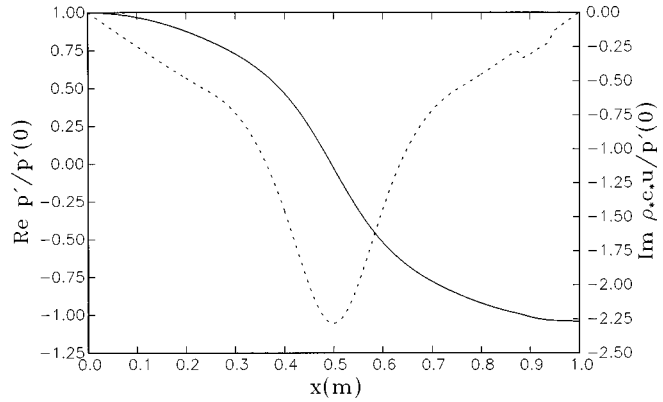

FIG. 14. Real part of the pressure eigenfunction (solid line, left vertical scale) and imaginary part of the normalized velocity eigenfunction (dashed line, right vertical scale) for a thickening tube with $C=-0.2$; $\Delta T=350$ K and $p_0=500$ kPa.

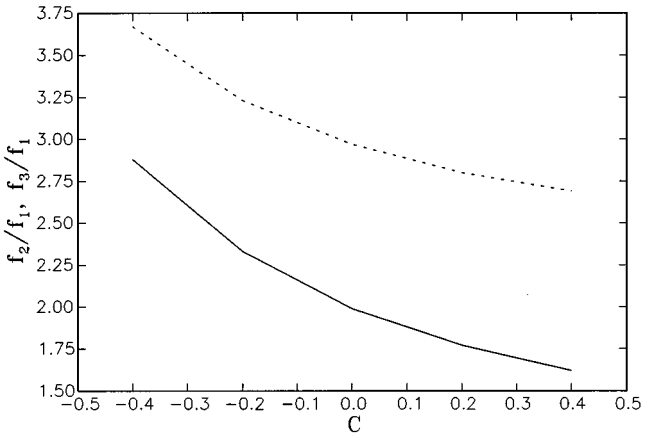

FIG. 15. Ratios f_2/f_1 (solid line) and f_3/f_1 of the first and second harmonic frequencies to the fundamental as a function of the cross-section parameter C, Eq. (79) for $\Delta T=300$ K, $p_0=500$ kPa. Positive C corresponds to an area increase.

result in a considerable detuning, with contractions relatively more effective than expansions.

VI. CONCLUSIONS

We have presented an approximate theory of a thermoacoustic prime mover based on a quasi-one-dimensional approximation. Primarily, the theory differs from available ones in the following respects:

(1) It is nonlinear in nature.

(2) It is formulated in the time domain.

(3) It can readily account for changes of the device's cross section in the direction normal to the wavefronts also in the nonlinear case.

This paper has dealt with the linear version of the model and has shown that, in those situations where the exact theory available in the literature applies, the approximate theory gives results for the pressure eigenfunctions and frequency eigenvalues that are identical to the exact ones. The cross-sectional averages of the other primary fields—velocity, temperature, and density—are reproduced exactly, but not the pointwise structure in the cross section. As a consequence, the mean value of fields nonlinear in the primary ones, such as the energy flux, is not reproduced exactly in the model. A preliminary analysis given in Sec. IV would seem to indicate that this error is not serious in many cases.

We have applied the theory to data that had, in the past, only been examined on the basis of an approximate model and we have found a very good agreement. We have also shown some results for tubes of axially varying cross section finding a tendency to greater instability for a tube that widens in its midsection.

The present model can be made more realistic by including heat conduction in the stack and other effects. Furthermore, it can equally well be adapted to the refrigerator case. Work in these directions is currently under way.

The study of the nonlinear regime with the present model still remains a rather complex matter and will be carried out in subsequent papers. Some results are shown in Part II of this work (Yuan *et al.*, 1997).

ACKNOWLEDGMENTS

The original idea to develop a quasi-one-dimensional model was suggested by Professor Lev Ostrovsky to whom the authors express their gratitude. Thanks are also due to the referees and to the Office of Naval Research for support of this study.

Achard, J. L., and Lespinard, G. M. (**1981**). ''Structure of the transient wall-friction law in one-dimensional models of laminar pipe flows,'' J. Fluid Mech. **113**, 283–298.

Arnott, W. P., Bass, H. E., and Raspet, R. (**1991**). ''General formulation of thermoacoustics for stacks having arbitrarily shaped pore cross sections,'' J. Acoust. Soc. Am. **90**, 3228–3237.

Arnott, W. P., Bass, H. E., and Raspet, R. (**1992**). ''Specific acoustic impedance measurements of an air-filled thermoacoustic prime mover,'' J. Acoust. Soc. Am. **92**, 3432–3434.

Arnott, W. P., Lightfoot, J. A., Raspet, R., and Moosmüller, H. (**1996**). ''Radial wave thermoacoustic engines: Theory and examples for refrigerators and high-gain narrow-bandwidth photoacoustic spectrometers,'' J. Acoust. Soc. Am. **99**, 734–45.

Atchley, A. A. (**1992**). ''Standing wave analysis of a thermoacoustic prime mover below onset of self-oscillation,'' J. Acoust. Soc. Am. **92**, 2907–2914.

Atchley, A. A. (**1994**). ''Analysis of the initial build-up of oscillations in a thermoacoustic prime mover,'' J. Acoust. Soc. Am. **95**, 1661–1664.

Atchley, A. A., and Kuo, F. M. (**1994**). ''Stability curves for a thermoacoustic prime mover,'' J. Acoust. Soc. Am. **95**, 1401–1404.

Atchley, A. A., Bass, H. E., and Hofler, T. J. (**1990a**). ''Development of nonlinear waves in a thermoacoustic prime mover,'' in *Frontiers in Nonlinear Acoustics*, edited by M. F. Hamilton and D. T. Blackstock (Elsevier, New York), pp. 603–608.

Atchley, A. A., Bass, H. E., Hofler, T. J., and Lin, H.-T. (**1992**). ''Study of a thermoacoustic prime mover below onset of self-oscillation,'' J. Acoust. Soc. Am. **91**, 734–743.

Atchley, A. A., Hofler, T. J., Muzzerall, M. L., Kite, M. D., and Ao, C. (**1990b**). ''Acoustically generated temperature gradients in short plates,'' J. Acoust. Soc. Am. **88**, 251–263.

Chapman, S., and Cowling, T. G. (**1952**). *Mathematical Theory of Nonuniform Gases* (Cambridge U.P., Cambridge, England), 2nd ed.

Crocco, L. (**1958**). ''One-dimensional treatment of steady gas dynamics,'' in *Fundamentals of Gas Dynamics*, edited by H. W. Emmons (Princeton U.P., Princeton, NJ), pp. 64–349.

Gaitan, D. F., and Atchley, A. A. (**1993**). ''Finite amplitude standing waves in harmonic and anharmonic tubes,'' J. Acoust. Soc. Am. **93**, 2489–2495.

Landau L. D., and Lifshitz, E. M. (**1959**). *Fluid Mechanics* (Pergamon, London).

Merkli, P., and Thomann, H. (**1975**). ''Thermoacoustic effects in a resonance tube,'' J. Fluid Mech. **70**, 161–177.

Olson, J. R., and Swift, G. W. (**1994**). ''Similitude in thermoacoustics,'' J. Acoust. Soc. Am. **95**, 1405–1412.

Press, W. H., Vetterling, W. T., Teukolsky, S. A., and Flannery, B. P. (**1992**). *Numerical Recipes in FORTRAN* (Cambridge U.P., Cambridge, England), 2nd ed.

Raspet, R., Bass, H. E., and Kordomenos, J. (**1993**). ''Thermoacoustics of traveling waves: Theoretical analysis for an inviscid ideal gas,'' J. Acoust. Soc. Am. **94**, 2232–2239.

Rott, N. (**1969**). ''Damped and thermally driven acoustic oscillations in wide and narrow tubes,'' Z. Angew. Math. Phys. **20**, 230–243.

Rott, N. (**1975**). ''Thermally driven acoustic oscillations, Part III: Second-order heat flux,'' Z. Angew. Math. Phys. **26**, 43–49.

Rott, N. (**1976**). ''Thermally driven acoustic oscillations, Part IV: Tubes with variable cross section,'' Z. Angew. Math. Phys. **27**, 197–224.

Rott, N. (**1980**). ''Thermoacoustics,'' Adv. Appl. Mech. **20**, 135–175.

Rott, N. (**1983**). ''Thermally driven acoustic oscillations, Part VI: Excitation and power,'' Z. Angew. Math. Phys. **34**, 609–626.

Swift, G. W. (**1988**). ''Thermoacoustic engines,'' J. Acoust. Soc. Am. **84**, 1145–1180.

Swift, G. W. (**1992**). ''Analysis and performance of a large thermoacoustic engine,'' J. Acoust. Soc. Am. **92**, 1551–1563.

Tominaga, A. (**1995**). ''Thermodynamic aspects of thermoacoustic theory,'' Cryogenics **35**, 427–440.

Vargaftik, N. B. (**1975**). *Handbook of Physical Properties of Liquids and Gases* (Wiley, New York).

Wheatley, J. (**1986**). ''Intrinsically irreversible or natural heat engines,'' in Frontiers in Physical Acoustics, edited by D. Sette (North-Holland, Amsterdam), pp. 35–475.

Wheatley, J., Hofler, T., Swift, G. W., and Migliori, A. (**1983**). ''An intrinsically irreversible thermoacoustic engine,'' J. Acoust. Soc. Am. **74**, 153–170.

Whitham, G. B. (**1974**). *Linear and Nonlinear Waves* (Wiley, New York).

Yazaki, T., Takashima, S., and Mizutani, S. (**1987**). ''Complex quasiperiodic and chaotic states observed in thermally induced oscillations of gas columns,'' Phys. Rev. Lett. **58**, 1108–1111.

Yazaki, T., Tominaga, A., and Narahara, Y. (**1980**). ''Experiments on thermally driven acoustic oscillations of gaseous helium,'' J. Low Temp. Phys. **41**, 45–60.

Yuan, H., Karpov, S., and Prosperetti, A. (**1997**). ''A simplified model for linear and nonlinear processes in thermoacoustic prime movers. Part II. Nonlinear oscillations,'' J. Acoust. Soc. Am. **102**, 3497–3506.